International Communications in Heat and Mass Transfer 48 (2013) 80–85

Contents lists available at ScienceDirect

International Communications in Heat and Mass Transfer

journal homepage: www.elsevier.com/locate/ichmt

Thermoelectric transformation and illuminative performance analysis of a novel LED-MGVC device ☆

Jung-Chang Wang *

Department of Marine Engineering, National, Taiwan Ocean University (NTOU), Keelung 20224, Taiwan, ROC

ARTICLE INFO

Available online 7 September 2013

Keywords:
LED
Vapor chamber
Thermoelectric
TGM
Performance
Illumination
MGVC
VCPCB

ABSTRACT

Energy-efficient, small and lightweight high-power light-emitting diodes (Hi-LEDs) are combined with a thermo-generation module (TGM) to transform the heat power generated by the LED into electric energy in the present paper. Variation in the dielectric copper and solder layer thickness in the printed circuit board (PCB) composite was found to affect the thermal performance of the Hi-LEDs lighting system, and a vapor chamber (VC) was shown to provide excellent heat dissipation performance when used with Hi-LEDs. Therefore, VC and PCB (VCPCB) were combined for integration with the Hi-LEDs package system (micro-generator with LED vapor chamber-based plate, LED-MGVC) for performance and illumination comparison. This study analyzes the performance of a novel LED-MGVC device using experimental and illumination-analysis methods with VCTM V1.0. Results depict that the LED-MGVC system provides significant improvement for thermal performance and illumination and thermoelectric properties.

1. Introduction

Compared with traditional incandescent lamps, high-power light-emitting diodes (Hi-LEDs) technology presents significant benefits over traditional incandescent lamps and has thus begun to be aggressively used in lighting applications including street lamps, traffic lights, automobile headlights, backlights for liquid crystal display (LCD) televisions, building lighting and indoor-lighting lamps. Although LEDs are considerably more efficient than traditional lighting (15–25% vs. 10%), Hi-LEDs still produce a significant amount of heat flow during operation [1–3]. Thus, as high-power LED arrays are used more widely for general lighting systems, they generate a more significant amount of heat flux (above 85 %). LEDs can be classified as high brightness and general brightness, with high-brightness and high-power LEDs usually producing more than 1 W of heat per die. The power package of a single LED die has a surface area of 1 mm^2, with a total heat power of 1 W. Thus, a single high-power LED usually has a heat flux greater than 100 W/cm^2. This heat flux easily results in thermal hot spots at the device junction, thus reducing the life span of high-brightness LEDs.

A vapor chamber is a two-phase heat transfer component that uniformly spreads and transfers heat flow, making it ideal for use in non-uniform heating conditions such as in Hi-LEDs. The effectiveness and improved thermal performance of vapor chambers has been confirmed in prior studies through mass application in server systems and VGA thermal modules [4–6]. Wang and Wang [7] derived a novel formula for the effective thermal conductivity of vapor chambers by use of modified dimensional analysis combined with a thermal-performance experimental method. Results show that its effective thermal conductivity increases with input power above 800 W/m°C, with a margin of error of less than ± 5 %. Wang et al. [8] reported a thermal-performance experiment using the illumination-analysis program VCTM V1.0 to discuss green illumination techniques using LEDs as a solid-state luminescence source in light lamps with the application of a vapor chamber to 30 W Hi-LEDs. Virtual Basic V6.0 was used to code the theoretical models with empirical formulae for computer-aided modeling thermal modules to develop the VCTM V1.0 program for convenient use in industrial applications. A thermoelectric generating module (TGM) is making use of the Seeback effect to convert the heat flow into electric energy through the use of thermoelectric materials [9–18]. Francisco et al. [19] utilized thermoelectric generators (TEG) and heat pipe (HP) modules based on the Seebeck effect to transform waste heat into electric energy for low (15 kW) and a high (40 kW) operating modes. Results demonstrated the potential of this system for recovering otherwise wasted heat. Kagawa et al. [20] applied a thermoelectric generator/thermo-generator to a municipal solid waste incinerator to capture low temperature thermal energy. Nevertheless, a micro-generator with LED vapor chamber-based plate (LED-MGVC) device combining LED-VCPCB [21] with TGM is shown to reduce the LED hot-spot problem and produce high levels of lighting energy efficiency.

This article uses computer-aided modeling design tools to analyze LED-MGVC performance, as shown in Fig. 1. A TGM is put on a LED vapor chamber-based plate, and the heat generated by the LED is stored in the lithium-ion battery through the Seebeck effect. It is important to use proper CAD/CAE tools in LED-MGVC design, and appropriate thermal

☆ Communicated by W.J. Minkowycz.

* Corresponding author at: No.2, Beining Rd., Keelung 20224 Taiwan, ROC.
E-mail address: jcwang@ntou.edu.tw.

0735-1933/$ – see front matter © 2013 Elsevier Ltd. All rights reserved.
http://dx.doi.org/10.1016/j.icheatmasstransfer.2013.08.008

Nomenclature

A	sectional area, m^2
I	electric current, A
K	thermal conductivity, W/m °C
L	length of thermoelectric element, meter
P	output energy, W
Q	heat transfer rate, W
R	thermal (or electrical) resistance, °C/W (or Ω)
T	temperature, °C
V	potential difference, V
W	width of thermoelectric element, m

Greek letters

α	Seebeck coefficient, V/K
η	ratio efficiency
π	Peltier coefficient, V
σ	material conductivity $(\Omega \cdot m)^{-1}$
τ	Thomson coefficient, W/K

Subscripts

A	air/ambient
C	cold side
h	hot side
N	N-type thermoelectric element
P	P-type thermoelectric element
eff	effective
in	input
LED-MGVC	micro-generator with LED vapor chamber-based plate
Out	output
TGM	thermo-generation module
Vc	vapor chamber

conditions were ensured through using a composite approach to LED-MGVC computer-aided modeling design. Several theoretical models for thermal modules have been developed, using software and algorithms to predict thermal, optical and electric performances in the computer-aided modeling design system, and the relevant programs and methods for computer-aided LED-MGVC design are introduced in the present paper.

2. Methodology

1. Performance analysis

Thermoelectric physical phenomena can take the form of external energy caused by temperature differences between objects to produce the potential difference for power generation. A thermoelectric power generation system must have a cold end and a hot end, with a load circuit (R_L) as shown in Fig. 2. The system operates on the basic principle of thermoelectric physical phenomena for thermoelectric semiconductors. The present study uses power generation chip analysis to analyze the thermoelectric transformation performance of LED-MGVC. LED-MGVC thermoelectric performance can be divided into the Seebeck, Peltier and Thomson effects. Eqs. (1)–(4) reveal their relational coefficients, including α, π and τ. The Seebeck effect indicates that two different metals connected in a closed loop will generate an electromotive force when the two metal contacts produce a temperature difference. The Peltier effect affects the current in a closed loop formed by the two different metals, where the physical phenomena of heat absorption and release form at both ends of the metal contacts in proportion to the amount of input current. The electromotive force of the thermoelectric power generation system is generated by the voltage addition due to the thermoelectric element within the circuit series, while the current flows through the load circuit output. The temperature difference between the cold and hot ends is due to the low thermal conductivity of the thermoelectric elements, preventing most of the heat capacity from being transmitted by the hot end to the cold side, thus maintaining the temperature difference. The merit of ZT is the judgment of thermoelectric materials, which is calculated in Eq. (5), where σ is the material conductivity of $(\Omega \cdot m)^{-1}$ and K is the thermal conductivity of W/mK. Therefore, a higher value of ZT indicates a high Seebeck coefficient and low thermal conductivity, resulting in the increased generation of thermoelectric power.

$$\alpha = -\frac{dV}{dT} \tag{1}$$

$$\pi = \frac{\left(\frac{dQ}{dT}\right)}{I} \tag{2}$$

$$\left(\frac{\pi}{\alpha}\right) = T \tag{3}$$

$$\left(\frac{\tau}{\alpha}\right) = I \tag{4}$$

$$ZT = \frac{\alpha^2 \sigma}{K} \tag{5}$$

The current value of the best performance of the power generation chip can be derived through the basic theory of thermoelectric physical effect and the Fourier heat transfer law, with the equivalent circuit for the power generation chip shown in Fig. 3. The voltage value V is generated by the thermoelectric power generation, R_i is the resistor generated by the thermoelectric material and R_L is the resistor compared with the applied load. According to the Seebeck effect, the voltage generated by the power generation chip is proportional to the chip temperature difference between the hot and cold sides following Eq. (6),

$$V = \alpha\left(\overline{Th} - \overline{Tc}\right) \tag{6}$$

where V is the electromotive force, α is the Seebeck coefficient of the materials, $\overline{Th}$ and $\overline{Tc}$ are the respective average temperatures of the hot and cold ends of the power generation chip.

The current I relationship of power generation chip is shown in Eq. (7),

$$I = \frac{V}{R} = \frac{\alpha \Delta T}{R_i + R_L} \tag{7}$$

According to the conservation of energy, the energy generated P by a power generation will be its power to the load R_L as shown in Eq. (8). Q_h and Q_c are the heat capacity of the hot and cold sides, as shown in Eqs. (9) and (10), respectively. These are divided into three parts for discussion: αITh is the thermoelectric effect, I^2R indicates the Joule heat, divided equally between the hot and cold sides, and $\frac{Ak(Th-Tc)}{L}$ is the Fourier effect of the heat flow from high to low temperature. The energy generated by the power generation chip P is less the heat to the cold side is the heat supply of the hot end ($Qh - Qc$), which is used to generate the load R_L. Thus, the output energy P is functional to current I as shown in Eq. (11). If the output energy P is differenced by the current I and is then set equal to zero, the power generation chip will produce the maximum output power P_{max} as shown in Eq. (12). The ratio efficiency η of thermoelectric power generation chip is shown in Eq. (13), and the

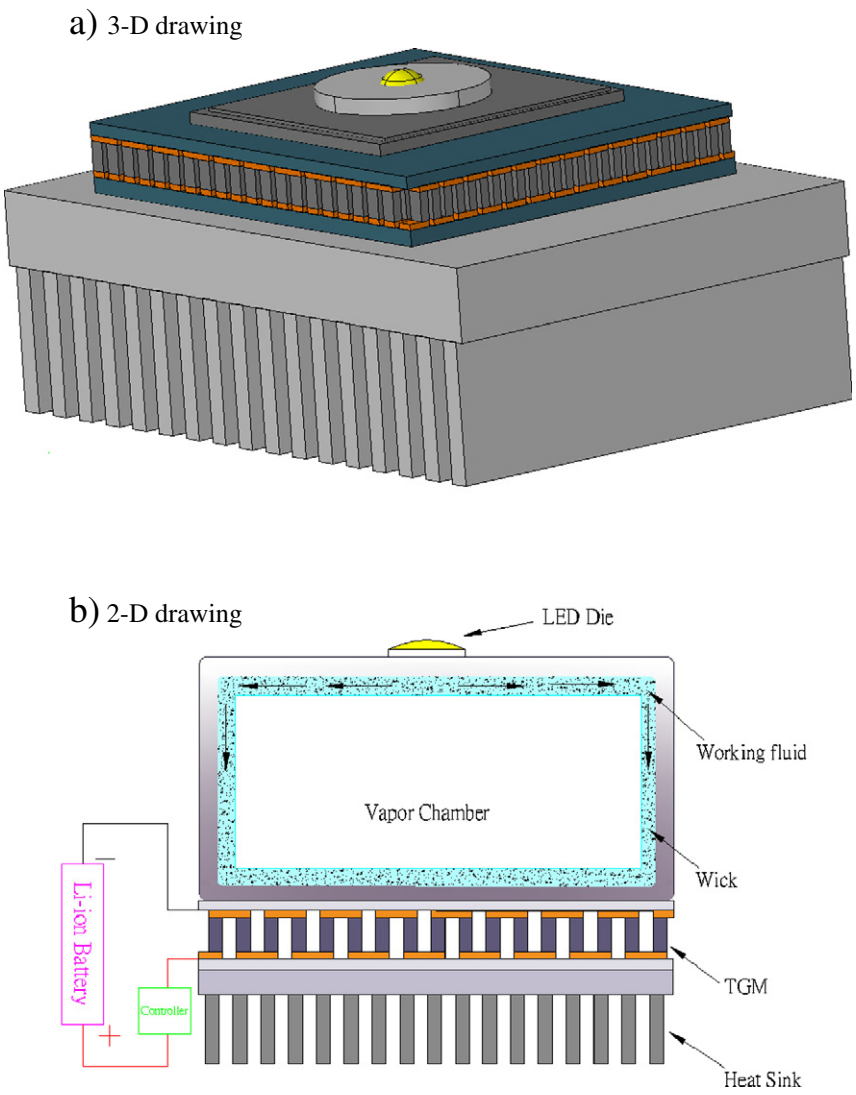

Fig. 1. Sketches of LED-MGVC: (a) 3-D drawing and (b) 2-D drawing.

performance value of the differential current I_η derived from Eq. (14) is the best current performance.

$$P = I^2 R_L \tag{8}$$

$$Q_h = \alpha I T_h - \frac{1}{2} I^2 R_L + \frac{Ak(T_h - T_c)}{L} \tag{9}$$

$$Q_c = \alpha I T_c + \frac{1}{2} I^2 R_L + \frac{Ak(T_h - T_c)}{L} \tag{10}$$

$$P = \alpha I \Delta T - I^2 R_L \tag{11}$$

$$P_{max} = \frac{\alpha^2 \Delta T^2}{4R_L} \tag{12}$$

$$\eta = \frac{P}{Q_h} = \frac{\alpha I \Delta T - I^2 R_L}{\alpha I T_h - \frac{1}{2} I^2 R_L + \frac{kA\Delta T}{L}} \tag{13}$$

$$I\eta = \frac{2R_L K \Delta T - \sqrt{4{R_L}^2 K^2 \Delta T^2 - 2\alpha^2 K R_L \Delta T^3 + 4\alpha^2 K R_L T_h \Delta T^2}}{\alpha \Delta T R_L - 2\alpha R_L T_h} \tag{14}$$

The performance of the thermal module with the vapor chamber can be determined within several seconds by using the final formula for the thermal-performance experimental method for VCTM V1.0 in Ref. [8]. Accurately estimating the effective thermal conductivity of the vapor chamber is very important for obtaining the thermal performance of vapor chamber-based thermal module. The dimension analysis of {F.L.T.θ.} in the Buckingham Π theorem can be used to derive the thermal performance empirical formula of the vapor chamber as shown in Ref. [8]. This VCTM version 1.0 was coded using Microsoft® Visual Basic™ 6.0 following the empirical Eq. (15) and is used here to calculate the thermal performance of a vapor chamber-based thermal module [8]. To avoid repetition, the calculations are not shown here. The LED-MGVC is designed and analyzed using VCTM V1.0 and 3-D numerical methods. For the entire module, about 500 thousands grid elements are used with about 2500 iterations, and simulating every scenario will take about 12 h.

$$k_{eff} = 46.1 \cdot (L_{vc} \cdot W_{vc})^{0.15} \cdot (t_{vc})^{0.24} \cdot (q_{in})^{0.28} \tag{15}$$

2. Experimental equipment and procedure

Fig. 4 shows the experimental apparatus and thermal resistance network of the LED-MGVC. The experimental procedure is divided into two tests. One is the thermoelectric performance of LED-MGVC with a range

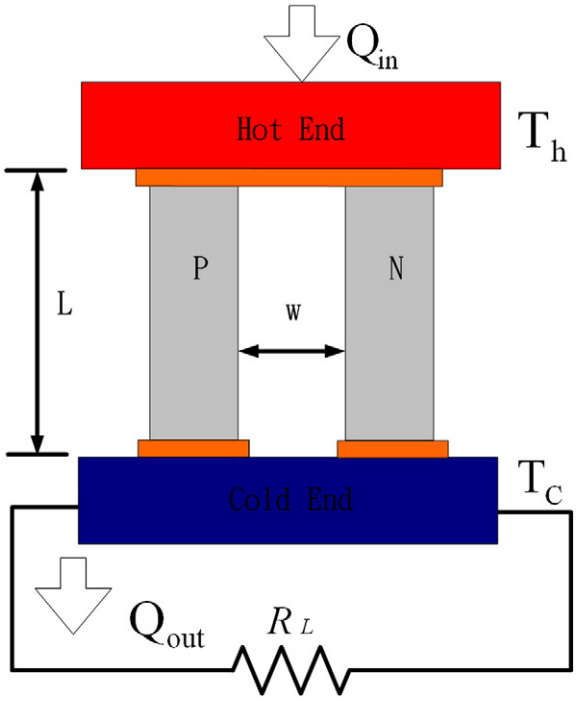

Fig. 2. Structure of a thermoelectric power generation system.

of input powers, and illumination of LED is another test. The LED-MGVC component contains the thermoelectric generator modules (TGM) and LED-VCPCB [21] and will absorb the waste heat produced by the LED temperature difference, transforming it into electrical energy and thus achieve optimal thermal management of high-power LED lighting modules. There are two types of LEDs lighting systems: type 1 has no vapor chamber, while and type 2 has a vapor chamber, and their performance is compared through thermal performance-illumination experiments of the energy storage system features using computer-aided modeling design with VCTM V1.0 to improve the illumination and life span of LED lights.

This experiment used an adjustable DC power supply for the LED lighting power that allowed calculation the input power, using model ADC50-10 with a power of 500 W, a maximum voltage of 50 V, a maximum current of 10 A and an error range of less than 0.5%. A T-type thermocouple made of copper–nickel–metal materials was used with a wire diameter of 0.25 mm, a measurement temperature range between −200 °C and 350 °C and an error range of ± 0.5 °C. A thermocouple spot welder soldering thermocouple spot manufactured by Taiwan Siong Kai (Mini-2K5A-1) was used for capacitor charge and discharge, using a welding electrode to weld the two wires together, with a welding wire diameter ranging between 0.1 mm and 1.0 mm. The GL-800 (Graphtec Systems, Japan) was used to record data measurements on 40 channels. Measurements including temperature, voltage, humidity, etc., can thus allowing data to be recorded to hard disk and output in an Excel spreadsheet with a maximum sampling time of 0.1 ms. A TES1330A digital display illuminometer was used with an illumination range of 0.01 lux to 20000 lux and an accuracy of ± 3%.

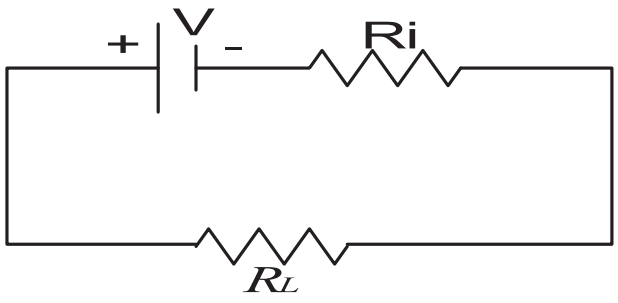

Fig. 3. The equivalent circuit for the power generation chip.

3. Results and discussions

Input power for the type 1 and type 2 modules was increased from 4 to 14 W in increments of 2 W, with the corresponding illumination observations summarized in Tables 1 and 2. LED input power at 4 W corresponded with 100% illumination. Increased input power to both modules was observed to correspond to the degree of illumination, and illumination performance was seen to depend on LED temperature for both systems. The experimental illumination results presented in Tables 1 and 2 show that the percentage of LED illumination does not increase with LED input power, and the contrast to the degree of increase in the percentage rate is much smaller than the LED relative input power percentage of increase. A maximum illumination of 3210 lux occurred at an LED input power of 8 W in type 1, while a maximum illumination of 3670 lux occurred at an LED input power of 10 W, with a maximum temperature of the two system modules reaching about 56 °C. Once the LED temperature exceeds 56 °C, illumination was found to decrease with further increases of LED input power due to increased temperatures. The intensity of LED luminosity was found to increase with temperature up to 56 °C, at which point LED illumination began to decay. As seen in the table, the illumination for the two modules begins to decline when LED temperatures exceed 56 °C, (specifically 55.9 °C for type 1 and 55.6 °C for type 2). The relative illumination with a vapor chamber for the type 2 module system was greater than that of the type 1 module system without a vapor chamber. The maximum contrast of the type 2 system was 166%, as opposed to 153% for the type 1 system. Therefore, although the increase in LED input power enhanced illuminance, at high temperatures, this illuminance begins to decay. Thus, in terms of LED input power, the increased margin of luminance per increase in input power is low, which presents a critical challenge for LED thermal management.

Fig. 5 compares the illumination of the type 1 and type 2 modules, showing that the type 1 module illuminance values are lower than that of the type 2 module, with an increase of LED input power to 10 W raising temperatures to 64.7 °C, at which point the illumination in the type 1 module began to decline to 3210 lux at 8 W and 1680 lux at 14 W. In contrast, the illumination value of the type 2 module began to trend downwards at 12 W with a corresponding LED temperature of 63.6 °C, dropping from 3670 lux at 10 W to 2100 lux at 14 W. The results indicate that at temperatures exceeding 56 °C LED illumination begins to degrade under the effects of heat stress. Finally, it can also be seen that the use of a vapor chamber in the type 2 module can effectively reduce the temperature of the LED and thus enhance LED illumination.

The waste heat produced by LED voltage and current can be recycled by power generation chips. Using the LED as the heat source, a temperature differential is formed between the hot and cold sides of the power chips, and this differential enables the chip to produce thermoelectric physical effects to generate electricity. Fig. 6 shows the thermoelectric chip current versus time in our experiments, with results indicating that the power generation chip's current reaches a steady state after about one minute. Following the path formation of power generation, output current was found to increase with time, with the current gradually reduced to a stable value with the LED input power of 4, 6, 8, 10, 12 and 14 W corresponding to 0.06, 0.08, 0.11, 0.13, 0.16 and 0.20 A. Poor thermal conductivity, mainly due to the thermoelectric element, resulted in a large temperature difference between the power generation chip's hot and cold junctions. Although the power generation chip can output

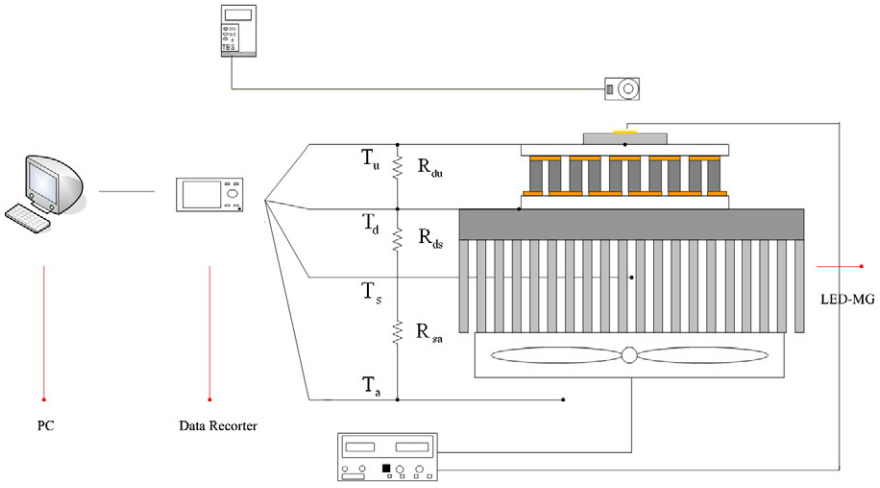

Fig. 4. Experimental apparatus and thermal resistance network of the LED-based plate.

a large current, compliance with energy conservation laws resulted in the temperature difference between the hot and cold sides gradually reducing to a stable value, and the experimental results were in line with theoretical understanding of the physical phenomena of thermoelectric power generation.

Fig. 7 compares the type 1 and type 2 module generation chip output current. According to manufacturer labeling, the thermoelectric material had a thermal conductivity resistance of 2.2 Ω for 1.6 W/mK, internal, and the Seebeck coefficient α was experimentally determined to be 0.0257 V/K. The generating chip output current of the two modules was seen to increase with the enhancement of the LED input power, specifically from 4 W 0.06 A to 0.14 A in the type 1 module, and from 4 W 0.06 A to 0.2 A in the type 2 module, both at 14 W. No significant difference was found between the module types at output current levels below 6 W, but at output current levels of about 6 W, the current of the type 2 module output was found to be higher than that of the type 1 module (0.11 vs. 0.10 A), and the type 2 slope was much larger than that of type 1. This is because, at high levels of input power, the vapor chamber can effectively transfer and spread heat capacity to the power generation chip, resulting in an increase in the chip's hot and cold side temperature difference. Therefore, the generation chip output current of the type 2 module resulted in a higher LED input power value.

Table 1
Relationships between LED input power and illumination for type 1.

Temperature (°C)	Illumination (lux)	Illumination percentage (%)	Input power (W)	Power percentage (%)
40	2100	100	4	100
48	2750	130.95	6	151.06
55.9	**3210**	**152.85**	**8**	**198.74**
64.7	2900	138.09	10	240.65
73.7	2090	99.52	12	295.89
82.6	1680	79.99	14	346.64

Table 2
Relationships between LED input power and illumination for type 2.

Temperature (°C)	Illumination (lux)	Illumination percentage (%)	Input power (W)	Power percentage (%)
37.4	2210	100	4	100
43.6	2900	131.22	6	151.06
50.1	3300	149.32	8	198.74
55.6	**3670**	**166.06**	**10**	**240.65**
63.6	3010	136.19	12	295.89
70.2	2100	95.02	14	346.64

4. Conclusions

This paper explores the power generation performance of two different LED module systems for power generation chips. Chip output power was found to increase with increase LED input power; with no significant difference between the two modules with LED input power of less than 6 W. As LED input power exceeded 6 W, the LED heat dissipation module with the vapor chamber was found to outperform the other LED cooling modules, with a maximum output power of 116.2 and 168 mW, respectively, for the type 1 and type 2 modules. The vapor chamber of the type 2 module generation chip was found to be superior to that of the type 1 module system with the non-uniform temperature plate. Mainly due to the vapor chamber under conditions of high heat flux, a higher heat transfer rate was obtained to rapidly conduct and dissipate heat from the LEDs to the surface of the power generation chip's hot end, and then to the cold end through the heat sink and cooling fan, thus transferring the heat to the air, resulting in the gradual increase of the temperature difference between the hot and cold sides of the generation chip. In addition, due to the LED heat conducting directly to the power generation chip, the LED heat dissipation MCPCB board cannot effectively conduct heat. In addition, the LED heat source area is smaller than that of the power generation chip, so most of the heat

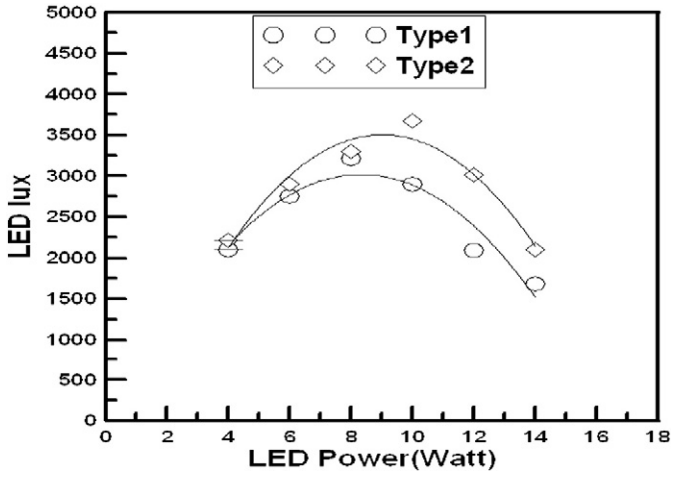

Fig. 5. Illumination comparisons for type 1 and type 2.

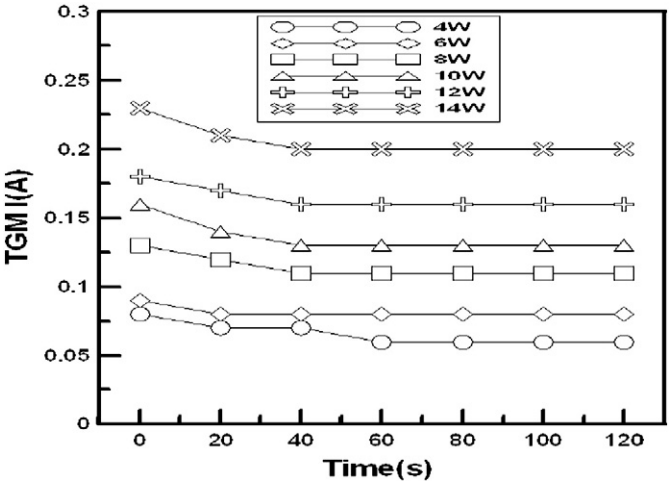

Fig. 6. Output Current with time for type 2.

is dissipated directly into the air, resulting in thermal resistance. Heat cannot be effectively transferred to the hot end of the power generation chip, thus decreasing the temperature difference between the hot and cold sides, resulting in the output of the power generation chip being inferior to that of the LED module with a vapor chamber.

However, in LED thermal management, about 80% of the electrical input power for high-power LED lighting will be wasted in the form of heat generated by the thermoelectric generating module (TGM). In evaluating the characteristics of micro-generator with LED vapor chamber-based plate (LED-MGVC) devices, this study finds that, given 6 W of input power, the heat source temperature of the LED-MGVC can be kept below 65 °C with a maximum illumination greater than 3200 lux and a maximum output power of 160 mW or more. The above conclusions indicate the selection of the LED heat dissipation substrate plays a vital role in the chip's power generation performance. The type 2 cooling modules has better energy storage characteristics than The type 1 module, thus making it possible to reduce the temperatures of more LED dies, thus allowing for increased illumination and life span.

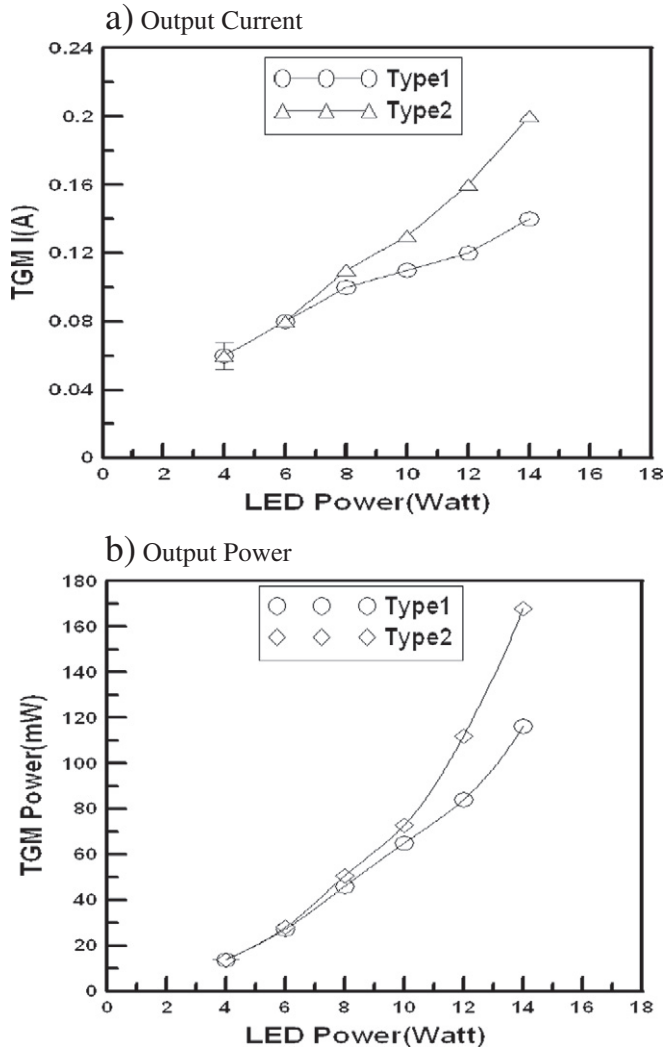

Fig. 7. Thermoelectric Transformations with LED input power for type 1 and type 2: (a) output current and (b) output power.

Acknowledgements

The author gratefully acknowledges the financial support from NSC 100-2221-E-019-064 and NSC 101-2221-E-019-042. The author also would like to thank all colleagues and students who contributed to this study.

References

[1] J.-C. Wang, Thermal investigations on LEDs vapor chamber-based plates, Int. Commun. Heat Mass 38 (9) (2011) 1206–1212.
[2] K. Gordon, Thermal Management of White LEDs, US Department of Energy, 2007. 1–2 (PNNL-SA-51901).
[3] J.-C. Shyu, K.-W. Hsu, K.-S. Yang, C.-C. Wang, Orientation effect on heat transfer of a shrouded LED backlight panel with a plate-fin array, Int. Commun. Heat Mass 42 (2013) 51–54.
[4] J.-C. Wang, Development of vapour chamber-based VGA thermal module, Int. J. Numer. Methods Heat 20 (4) (2010) 416–428.
[5] R.-T. Wang, J.-C. Wang, T.-L. Chang, Experimental analysis for thermal performance of a vapor chamber applied to high-performance servers, J. Mar. Sci. 19 (4) (2011) 353–360.
[6] J.-C. Wang, 3-D numerical and experimental models for flat and embedded heat pipes applied in high-end VGA card cooling system, Int. Commun. Heat Mass 39 (9) (2012) 1360–1366.
[7] J.-C. Wang, R.-T. Wang, A novel formula for effective thermal conductivity of vapor chamber, Exp. Tech. 35 (5) (2011) 35–40.
[8] J.-C. Wang, R.-T. Wang, T.-L. Chang, D.-S. Hwang, Development of 30 Watt high-power LEDs vapor chamber-based plate, Int. J. Heat Mass Transfer 53 (19/20) (2010) 3900–4001.
[9] X. Niu, J. Yu, S. Wang, Experimental study on low-temperature waste heat thermoelectric generator, J. Power Sources 188 (2009) 621–626.
[10] B. David, J. Ramousse, L. Luo, Optimization of thermoelectric heat pumps by operating condition management and heat exchanger design, Energy Convers. Manage. 60 (2012) 125–133.
[11] C.T. Hsu, G.Y. Huang, H.S. Chu, B. Yu, D.J. Yao, Experiments and simulations on low-temperature waste heat harvesting system by thermoelectric power generators, Appl. Energy 88 (2011) 1291–1297.
[12] A. Rezania, L.A. Rosendahl, S.J. Andreasen, Experimental investigation of thermoelectric power generation versus coolant pumping power in a microchannel heat sink, Int. Commun. Heat Mass 39 (8) (2012) 1054–1058.
[13] James W. Stevens, Performance factors for ground-air thermoelectric power generators, Energy Convers. Manage. 68 (2013) 114–123.
[14] F. Meng, L. Chen, F. Sun, Effects of temperature dependence of thermoelectric properties on the power and efficiency of a multielement thermoelectric generator, Int. J. Energy Environ. 3 (2012) 137–150.
[15] X. Chen, B. Lin, J. Chen, The parametric optimum design of a new combined system of semiconductor thermoelectric devices, Appl. Energy 83 (2006) 681–686.
[16] A. Rodríguez, J.G. Vián, D. Astrain, A. Martínez, Study of thermoelectric systems applied to electric power generation, Energy Convers. Manage. 50 (2009) 1236–1243.
[17] W.H. Chen, C.Y. Liao, C.I. Hung, A numerical study on the performance of miniature thermoelectric cooler affected by Thomson effect, Appl. Energy 89 (2012) 464–473.
[18] R. Ahiska, K. Ahiska, New method for investigation of parameters of real thermoelectric modules, Energy Convers. Manage. 51 (2010) 338–345.
[19] P.B. Francisco, J. Martins, L.M. Goncalves, R. Sousa, Modelling of thermoelectric generator with heat pipe assist for range extender application, 37th Annual Conference of the IEEE Industrial Electronics Society (IECON 2011), November, Melbourne, Australia, 2011.
[20] S. Kagawa, M. Sakamoto, N. Hirayama, A practical test of a Bi-Te thermoelectric waste heat generator system in an incinerator using oil for heat transfer, 8th International Conference on Thermoelectrics, 1999, pp. 321–324.
[21] J.-C. Wang, T.-S. Sung, W.-P. Chen, Hyper-generation LEDs VCPCB, microsystems, packaging, Assembly and Circuits Technology Conference, 2011 6th International, 2011, pp. 332–335, (IMPACT 2011).